

**H. Medellín<sup>1</sup>**  
Facultad de Ingeniería,  
Universidad Autónoma de San Luis Potosí,  
Avenida Manuel Nava No. 8,  
Zona Universitaria,  
78290, San Luis Potosí, México  
e-mail: hugoivanmc@uaslp.mx

**T. Lim**  
e-mail: t.lim@hw.ac.uk

**J. Corney**  
e-mail: j.r.corney@hw.ac.uk

**J. M. Ritchie**  
e-mail: j.m.ritchie@hw.ac.uk

**J. B. C. Davies**  
e-mail: b.j.davies@hw.ac.uk

Mechanical Engineering,  
Heriot-Watt University,  
Edinburgh EH14 4AS, Scotland,  
United Kingdom

# Automatic Subdivision and Refinement of Large Components for Rapid Prototyping Production

*The aim of the work presented in this paper is to enable production of large, complex components on rapid prototyping machines whose build volume is less than the size of the desired component. Such large components can be produced as fabrications if a suitable subdivision can be generated. In general, any component can be subdivided into smaller parts by an array of orthogonal planes, but the resulting shapes could have geometries that are difficult to produce accurately on many rapid prototyping systems. The system presented here creates a decomposition designed for both rapid prototyping and assembly. The proposed method considers potential manufacturing problems, and modifies the boundaries of individual parts, where necessary. Additionally, the system also generates complementary male/female (i.e., matching protrusion/depression) assembly features at the interface between the component parts in order to improve the integrity and assembly of the final component. To prove the functionality of the system, three components are analyzed at the end of this paper. [DOI: 10.1115/1.2753162]*

**Keywords:** rapid prototyping, object decomposition, 3DU, DFRP, AFG, assembly features

## 1 Introduction

Even though solid freeform fabrication technologies have unprecedented flexibility, they still have limitations that prevent designers from easily creating certain shapes. While the precise capabilities of layer manufacturing systems vary, certain generic classes of problems are common to all approaches. Table 1 attempts to summarize these reported failings [1–10], some of which are illustrated in Fig. 1. Consequently, the challenge of design for rapid prototyping (DFRP) is the condition of optimal shapes and structures to satisfy functional need, while ensuring manufacturability [1]. This issue has been addressed in several research works; for instance, a manufacturability evaluation system for both subtractive and additive production processes was presented in [2]. When applied to an additive system, the tool selects the build orientation to give the best surface finish for rapid prototyping (RP).

According to [4], there are two approaches to designing parts for automated processing: design by decomposition and design by composition. In the design by decomposition approach, a CAD model is decomposed into layers, or other shapes, which match manufacturing processes. An RP system decomposes CAD models into slices for layered manufacturing, but if a large component is meant to be produced in an RP system, the build size limitation of the system may require an additional decomposition of the model into subcomponents. In principle, this additional decomposition may appear to be dictated solely by the build size (i.e., subcomponents should satisfy the build size limitation of the particular RP system). However, as each subcomponent will be produced as an individual part, the decomposition of large components must also consider the issues of “Design for RP” presented in Table 1. An optimal decomposition would be one that satisfies the build size limitation of the system, that does not generate

additional manufacturing problems, and that does not affect the integrity of the entire prototype (dimensional accuracy, feature resolution, mechanical properties, surface quality, etc.). Table 2 lists some of the commercial rapid prototyping systems and their corresponding build sizes according to their manufacturers.

As an example of large components, consider the cylinder head (538 mm × 178 mm × 234 mm) model shown in Fig. 2(a), which is typically produced by casting. The dimensions of this component make it difficult or even impossible to produce on many commercial RP machines (see Table 2). However, the part could be modeled on small capacity RP systems if it is subdivided into several geometrically simpler, and smaller, 3D subcomponents, and then assembled to form the desired shape. While a brute force subdivision (e.g., by a lattice of evenly spaced planes) can be used to decompose the model (Fig. 2(b)), it may inadvertently produce variable results. In the worst case, the resulting components can contain features that give rise to the problems listed in Table 1 and, consequently, affect the manufacturability and quality of the final fabrication. Similar “intelligent” problems have been investigated by researchers in areas ranging from RP to architecture.

Automated subdivision and the study of slicing methods has become an important aspect of RP technologies. For example, Dolenc and Makela [11] used adaptive slicing to reduce the stair-step error when slicing from stereolithography (STL) files, with a method that determines the optimal cusp height as a criterion for slicing. Krause et al. [12] described a method in which the geometric model is decomposed into vertical segments and each segment is sliced independently, depending on the required surface quality. Guduri et al. [13] reported a method to directly slice solid CAD models to obtain accurate laser beam paths for fused deposition modeling (FDM). Rajagopalan et al. [14] generated a series of cross-sectional profiles by slicing nonuniform rational B-spline surfaces using the I-DEAS CAD system. Jun et al. [15] and Smith et al. [16] presented methods to slice freeform surfaces for RP and machining applications based on identifying characteristic surface contour points. A survey by Kulkarni et al. [17] provides further

<sup>1</sup>Corresponding author.

Contributed by the Computer-Aided Product Development (CAPD) Committee of ASME for publication in the JOURNAL OF COMPUTING AND INFORMATION SCIENCE IN ENGINEERING. Manuscript received October 19, 2006; final manuscript received March 13, 2006. Assoc. Editor: S. Gupta.

Table 1 Shape related limitation of Rapid Prototyping systems

Issue	Description
Cavities	Internal cavities are hard to form since it may be difficult to remove the support material from internal regions.
Distortion, shrinkage, and warping	RP processes that involve solidification can give rise to residual stresses. The size and effect of the associate strains are dictated by the geometry of the components.
Feature damage	The breaking away of support structure processes may damage small features of the part. For example, cusps or thin sections may distort or break, during the production, or post- processing, processes because of their poor strength.
Feature size	Features must not be too small, too closely spaced, or require accuracy beyond the technology's capabilities (e.g., 0.02 in. Stratasys 1650 machine [3]).
Overhangs	Overhanging features may affect the surface flatness (distortion). Large overhanging features may require supports, which may affect the part quality.
Surface finish	Material, build orientation, layer thickness, sloped surfaces, intricate features, and curved surfaces all affect the surface finish. It is defined in terms of surface roughness, surface flatness, and amount of support structures. The surface finish affects the post-processing work, dimensional accuracy, and functionality of parts.
Volume	The maximum size of the component is defined by the capability of the individual RP system (see Table 2).

insight to slicing methods and their application in layered manufacturing. Huang et al. [18] described a system for subdividing large moulds.

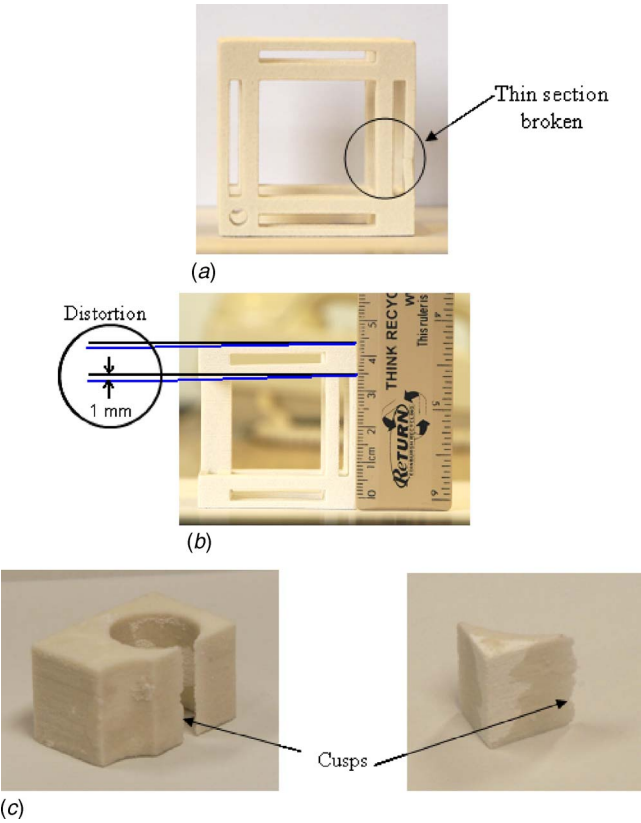


Fig. 1 Common problems in RP fabrication: (a) thin sections, (b) distortion, and (c) cusps

Table 2 Typical build sizes for midrange commercial RP systems

RP system	Build size
Z Corporation (Z310 printer)	200 mm × 250 mm × 200 mm
Stratasys (Prodigy Plus)	200 mm × 200 mm × 300 mm
3D systems (InVision 3D printer)	127 mm × 178 mm × 50 mm
3D systems (Viper si2)	250 mm × 250 mm × 250 mm
EOS systems (EOSINT M)	250 mm × 250 mm × 200 mm

Subdivision for machine tool manufacture provides a way to discretize the object model into simpler regions so that shape information can be processed automatically. Jun et al. [15] used the intrinsic topological changes on a freeform surface to develop a method for finding all intersection curves between the surface and a series of parallel planes. The results can be used downstream to generate numerical control (NC) tool paths. Smith et al. [16] implemented a surface-slicing scheme to generate tool paths for contour machining of freeform surfaces. Wang and Ravani [19] developed a subdivision algorithm to generate NC tool path for electric discharge machining. The method involves subdividing boundary curves of ruled surfaces such that pairs of curve seg-

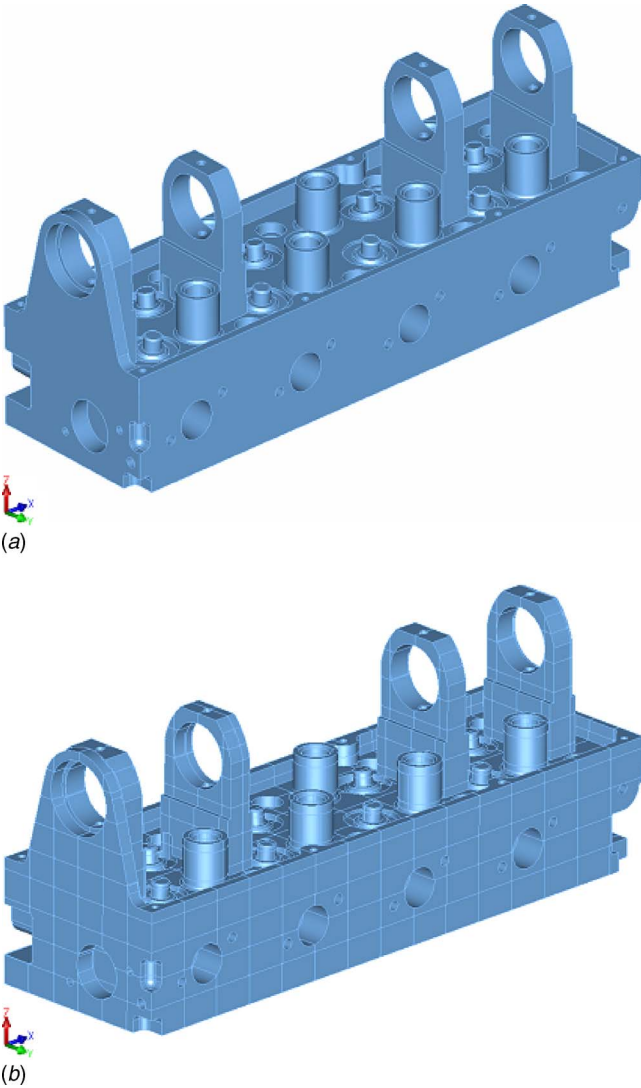


Fig. 2 Cylinder head: (a) the model and (b) regular lattice subdivision

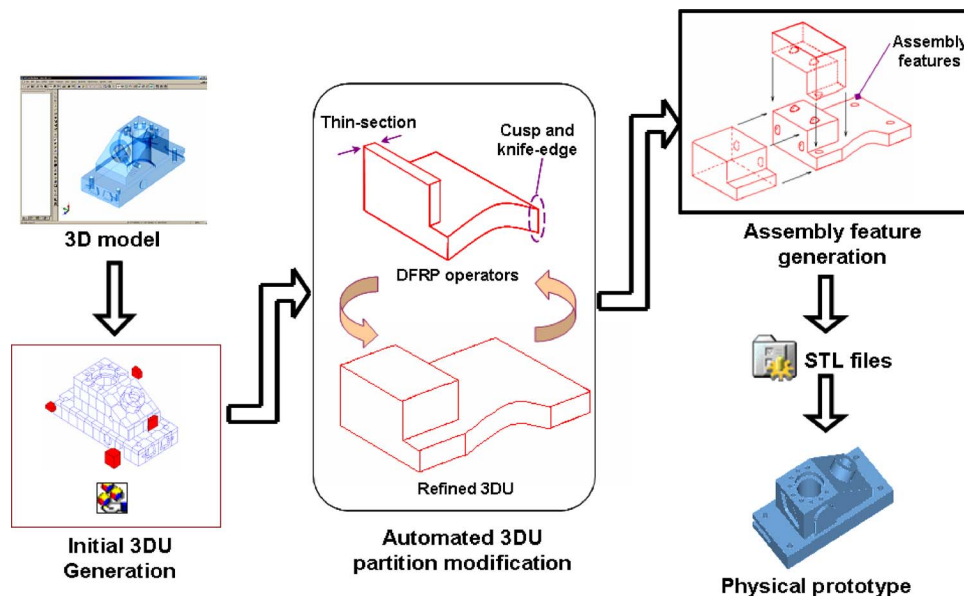


Fig. 3 Overview of 3DU-RP system

ments are within a flatness tolerance. The procedure also detects critical regions with small radii so that a revised tool path can be computed. More recently, Chan and Tan [20] reported a volume decomposition approach for CAD models to be produced in RP systems. The proposed approach subdivides models based on the volume limitations of RP systems, but does not consider other manufacturability problems, such as those shown in Table 1. The creation of physically large models from fabrications of RP produced components is also a particular concern in architecture. Consequently, recent work has discussed the application of design for assembly methodologies to the creation of large scale architectural models [21].

As an alternative to slicing up large CAD models into numerous thin sheets, a new approach is presented in this paper. The proposed system segments a 3D model into “3D units” (3DUs) of varying sizes and geometries. An iterative test-modify-and-test-again procedure for 3DU generation is used, where, based on the results of manufacturability tests, 3DUs are merged to resolve manufacturing problems. As part of the proposed decomposition approach, assembly features are generated on the contact faces of the 3DU set to improve the integrity and accuracy of the final component. The proposed system is described largely in the context of generating a subdivision oriented towards manufacturing large prototypes using standard RP systems (with build size and shape limitations), which has been considered as inappropriate due to the cost and machine speed of current processes [5]. Details of associated work on the decomposition of models, physical manufacture, and assembly of prototypes with regular and variable geometry have been reported in [22–27].

The rest of the paper is structured as follows: Sec. 2 gives an overview of the system; Sec. 3 describes the operators used to guide the partition refinement; Sec. 4 describes the generation of assembly feature process; Sec. 5 describes the implementation; Sec. 6 describes the results of applying the methodology to some test components; and last, Sec. 7 draws some conclusions and places the work in context.

## 2 System Overview

An overview of the proposed 3DU-RP system for the rapid prototyping of large components is presented in Fig. 3. This 3DU-RP system comprises:

1. A subdivision utility that creates an initial 3DU set.

2. Design for RP (DFRP) operators that modify this initial decomposition on the basis of geometric tests that detect potential manufacturing difficulties.
3. An assembly feature generator (AFG) that creates unique pairs of male/female matching features between the 3DUs to add location during fabrication (e.g., gluing) and improve the mechanical properties of the entire component.
4. Generation of STL files of the 3DU set for RP production.

The system works by first subdividing the component with a regular 3D lattice (Fig. 4(a)), then the manufacturability for RP production of the resulting 3DU set is assessed using three discrete functions referred to as DFRP operators. These operators perform geometric tests to identify the presence of features known to cause RP problems, such as thin sections, cusps, and knife edges (Fig. 4(b)). Depending on the problem identified, partitioning boundaries are modified by selective merging of adjacent 3DUs.

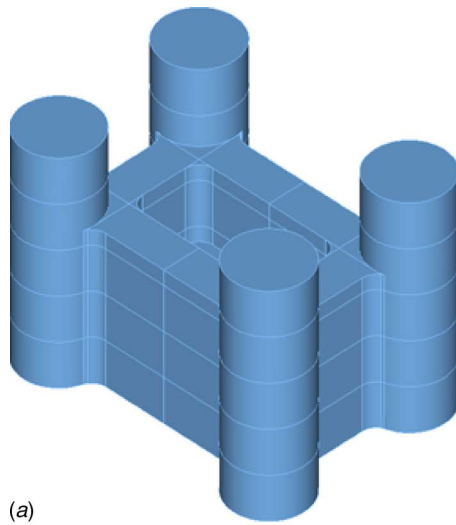
The process of refining the decomposition is iterative, and each DFRP operator can be applied several times as follows:

1. Application of DFRP operators to identify RP manufacturability problems (thin sections, cusps, knife edges, and undersized 3DUs).
2. Refinement of partition boundaries by selective merging.
3. Review and repeat steps 1–2, as required.

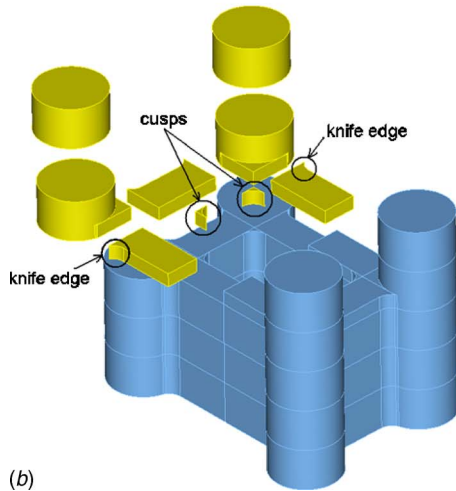
Once the component has been decomposed into a “feasible” 3DU set, the user can apply an AFG operator, which identifies contact faces among 3DUs to create male/female assembly features on them. The aim of the assembly features is to add location of parts during the assembly, and to improve the mechanical properties of the entire component. The number and location of the features depend on the dimension, shape, and location of the contact face. Figure 5 shows an example of assembly features created on the interface faces of 3DUs. The precise location of each set of features is randomly varied by a small amount to ensure that each 3DU has a unique mate. This guarantees that in a large assembly with many similar components, each 3DU can only be located in a unique position in the final fabrication.

When the generation of the assembly features has been completed, the set of 3DUs is ready to be fabricated, and therefore the next stage in the system is the generation of the STL files of the





(a)



(b)

**Fig. 4 Castle component: (a) 3D lattice decomposition and (b) identification of manufacturing problems in resultant 3DUs**

individual 3DUs to be produced in a RP system. Finally, the manual assembly of the 3DUs will produce the final component.

### 3 Design for RP Operators (DFRP)

Traditionally, manufacturability analysis has been applied to entire components to enable potential manufacturing problems to be identified during the design phase [28–30]. In contrast, the 3DU-RP system employs three DFRP operators to evaluate and, where necessary, modify the partition boundaries of individual 3DUs. The DFRP operators use selective merging functions for

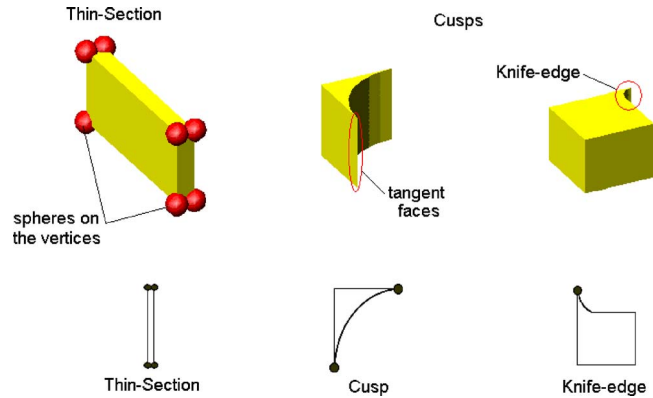


**Fig. 6 RP problems detected by the DFRP operators**

3DU boundary refinement. Merging is performed by the removal of internal faces that define the 3DU boundary. The selection of the 3DUs to merge is directly determined by the presence of manufacturing problems. The three DFRP operators are named Op\_thin, Op\_cusp, and Op\_vol.

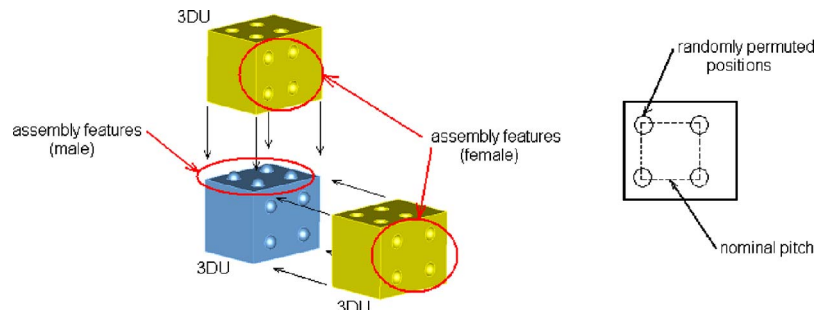
**Thin-Section Operator (Op\_thin).** Thin sections (TS) are detected by positioning spheres (default 1.5 mm radius) on all the vertices of the 3DU to test for intersections (Fig. 6). When any pair of vertex spheres intersects, a thin section is deemed to exist. The vertex sphere test has proved to be sufficiently robust to establish the feasibility of the proof-of-concept system reported here. The operator responds by selective merging of adjacent 3DUs.

**Cusp Operator (Op\_cusp).** Cusps (CP) are found by evaluating the local geometry adjacent to an edge. This classification examines both the type and tangent relationships between faces meeting at an edge, as illustrated in Fig. 6. The operator responds by selective merging of adjacent 3DUs.

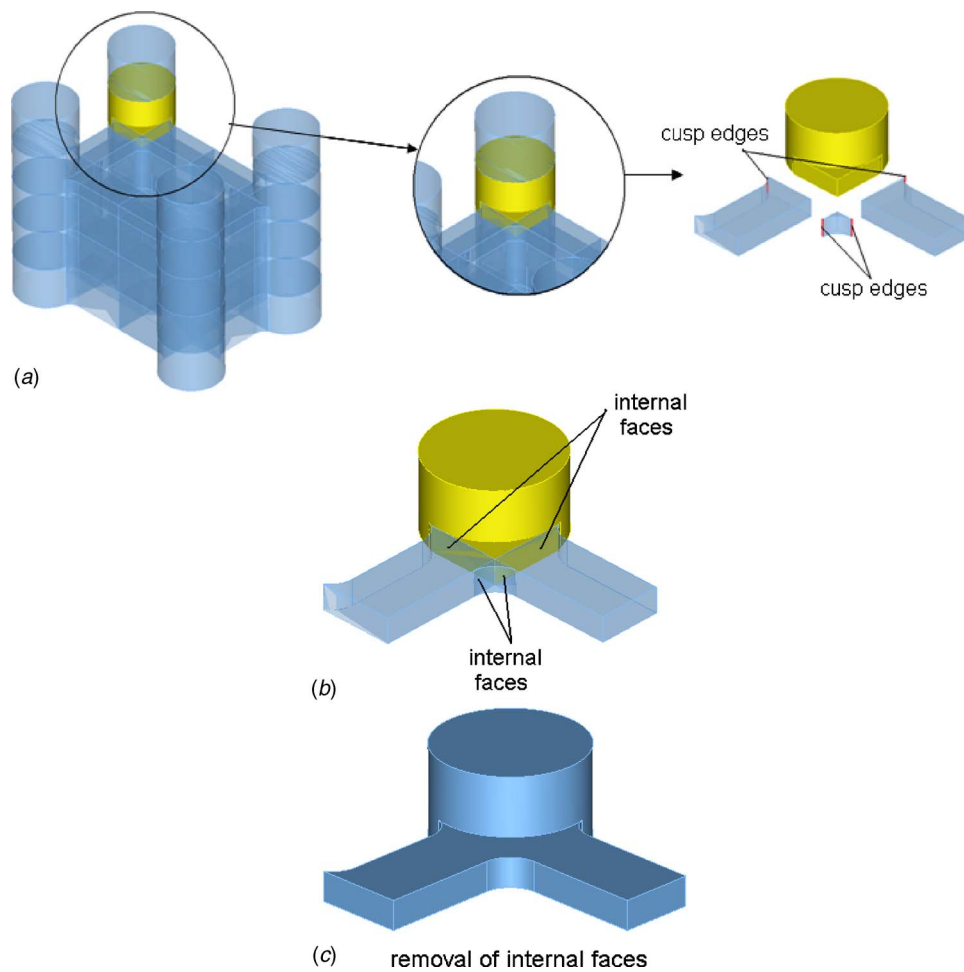
**Undersized Volume Operator (Op\_vol).** This operator detects undersized volumes (UV) of 3DUs, i.e., small 3DUs, by querying the mass properties of each unit and comparing the value to a threshold defined according to the characteristics of the RP system being used (default minimum volume 15 mm × 15 mm × 15 mm). The operator responds by selectively merging the 3DU.

Figure 7 illustrates the actions of the DFRP operators with some 3DUs from the “castle” component of Fig. 4. Figure 7(a) shows some problems identified by the Op\_cusp operator that result from the tangent relationship of the slicing plane to a circular curve, forming cusps. These problems are solved by identifying and removing the internal faces that separate these features from adjacent 3DUs (Figs. 7(b) and 7(c)).

The application of the DFRP operators may solve some prob-



**Fig. 5 Assembly features created on the 3DU faces**



**Fig. 7 Procedures for correcting DFRP issues: (a) RP problems, (b) identifying internal faces, and (c) merging of 3DUs to remove the problem**

lems by merging the 3DUs, but some new problems may arise in the new set of 3DUs. For this reason, the DFRP operators may be applied repeatedly as required.

#### 4 Assembly Feature Generation (AFG)

Once the final 3DU set has been obtained, assembly features are created using an operator that determines the size, number, and location of pairs of male/female features between individual 3DUs.

**Assembly Feature Operator (Op\_feature).** This operator creates assembly features on the interface (contact) surfaces shared

by 3DUs. Spherical features are used, and the size, number, and location of the features depend on the shape and dimensions of the contact area. Large areas require more and bigger assembly features to improve the integrity and alignment of the assembly. The Op\_feature operator comprises five steps (Fig. 8):

1. Locate interface (i.e., shared) faces between 3DUs.
2. Determine surface parameter range and divide it by the diagonal length of a box bounding the surface to determine the number of spheres to be generated.
3. Generate a pattern of spheres over parameter range, spaced according to the surface  $u$  and  $v$  parameter lines.

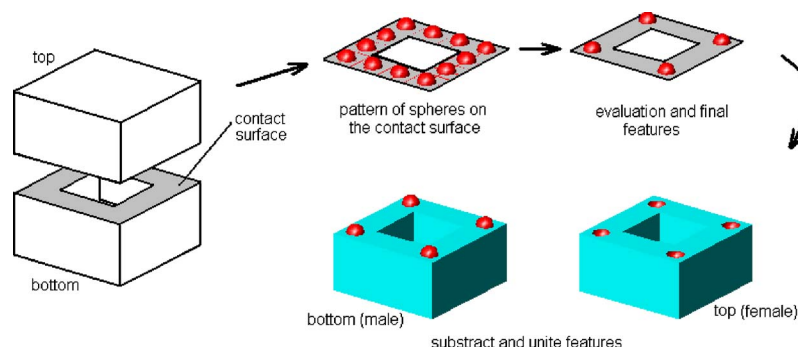


**Fig. 8 Generation of assembly feature process**

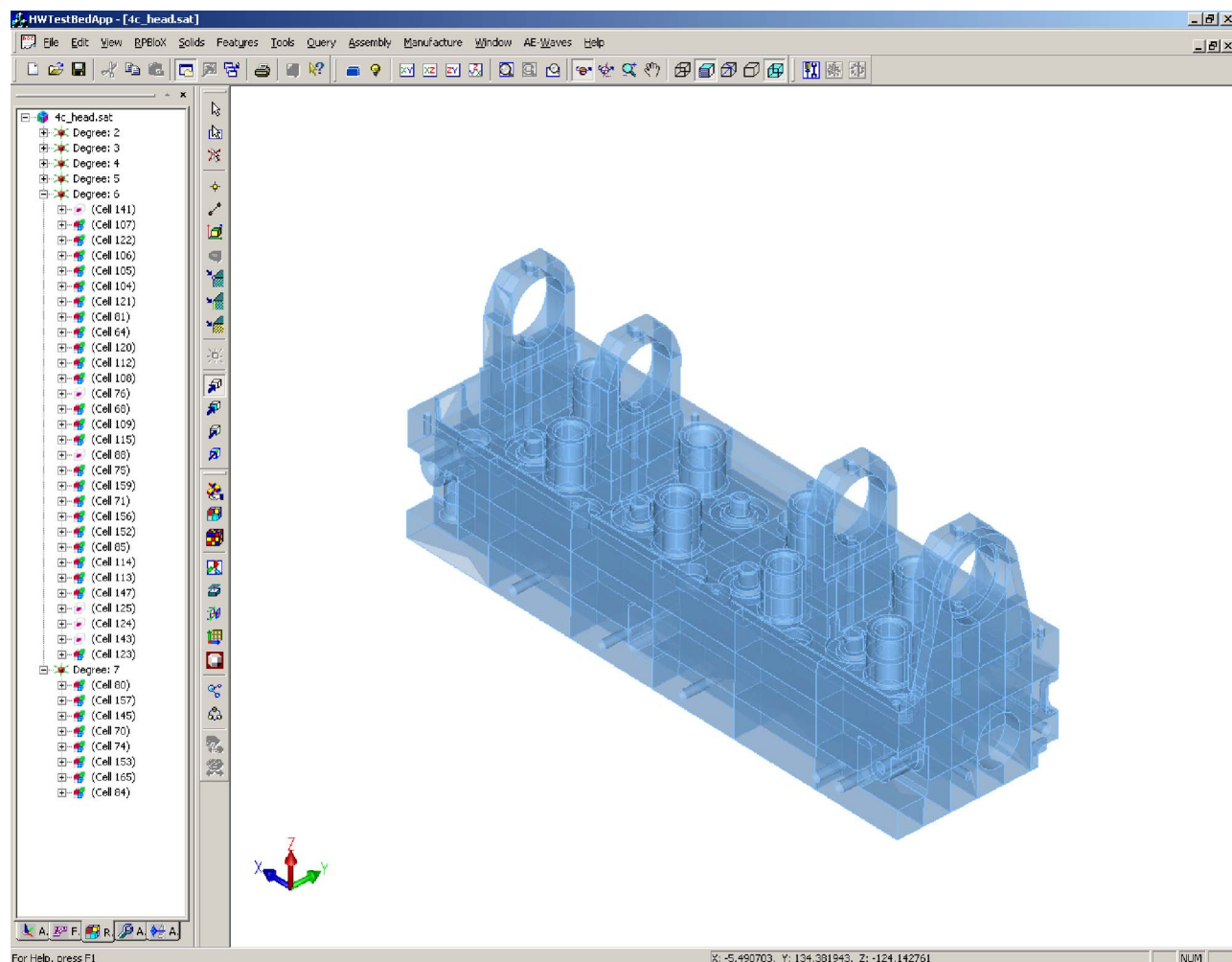


Fig. 9 The 3DU-RP system interface

4. Test sphere occupancy. Discard spheres that lie outside the surface and those whose hemispheres do not fully interact with the surface.
5. Subtract/unite spheres to the 3DUs in question.

In the current implementation, the pattern generated in step 3 is randomly permuted to ensure that each pair of assembly features is unique. Although it is possible to generate more complex as-

Table 3 DFRP results for test components

Lattice resolution		Castle											
		DFRP analysis				DFRP refinement							
						Optimization 1				Optimization 2			
						3DU set	TS	CP	UV	3DU set	TS	CP	UV
3 × 3 × 3	56	0	48	0	19	0	11	0	19	0	11	0	0
4 × 4 × 4	114	0	60	0	80	0	33	0	80	0	33	0	0
5 × 5 × 5	152	0	76	0	81	0	17	0	81	0	17	0	0
Truck													
3 × 3 × 3	60	24	24	36	40	15	6	0	38	15	6	0	0
4 × 4 × 4	112	22	28	2	83	11	14	0	83	11	14	0	0
5 × 5 × 5	190	29	42	0	136	20	16	0	136	20	16	0	0
Cylinder head													
3 × 3 × 3	74	18	71	14	64	13	61	22	42	11	40	0	0
4 × 4 × 4	128	34	118	27	78	8	68	7	60	5	54	0	0
5 × 5 × 5	180	60	140	60	137	42	111	9	86	10	62	0	0

Number of 3DUs with thin section (TS), cusp (CP), undersized volume (UV).

sembly features [31], the bump patterns have been proved sufficient to support the manual assembly of nonfunctional prototypes.

## 5 Data Structure and Implementation

To explore the subdivision and refinement strategies, a user interface has been developed using Visual C++ and ACIS® geometric modeling kernel [32]. Figure 9 presents the 3DU-RP system's unified interface, which allows interactive exploration of 3DUs via a tree control. This interface allows the subdivision operators to be applied automatically or manually. Manual subdivision and merging utilities let the users intervene in the refinement process when necessary. The system uses the cellular topology (CT) component of ACIS® to represent the subdivided solid CAD model. CT allows the modeling of subregions in a solid, and cells can be either 2D sheets or 3D solids. The DFRP and AFG operators work directly on the CT data structure. For example, cusps and thin sections are removed by unhooking internal face(s) that lie between adjacent cells causing the two volumes to be merged into one. Unique information is associated with each 3DU in the form of "attributes" supported by the kernel modeler. Examples of the type of information stored include the center of gravity, mass properties and spatial adjacency, geometry, and topology.

## 6 Results and Discussion

The results of the decomposition process depend on the initial slicing lattice resolution, orientation, and how the DFRP operators are applied. By default, the system uses a  $3 \times 3 \times 3$  lattice resolution.

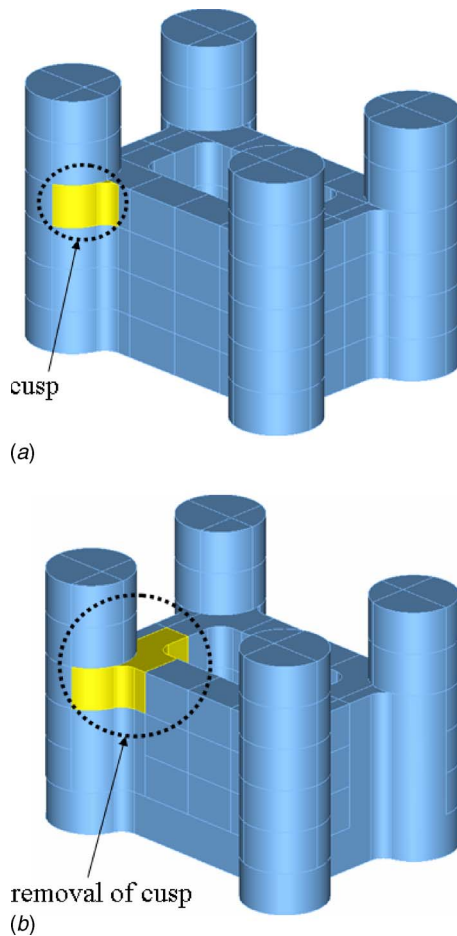


**Fig. 10** Partition refinement for the castle component with a  $5 \times 5 \times 5$  lattice resolution: (a) before refinement (152 3DUs) and (b) after refinement (81 3DUs)

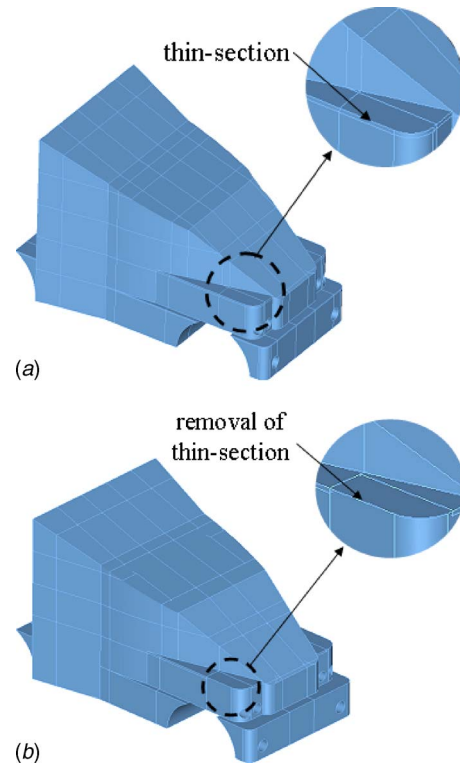


**Fig. 11** Partition refinement for the truck with a  $4 \times 4 \times 4$  lattice resolution: (a) before refinement (112 3DUs) and (b) after refinement (83 3DUs)

tion, but the user has the option to set another resolution that may avoid manufacturing problems. The DFRP operators can remove the majority of manufacturing problems, but the adaptive decomposition process cannot fix two types of issues:

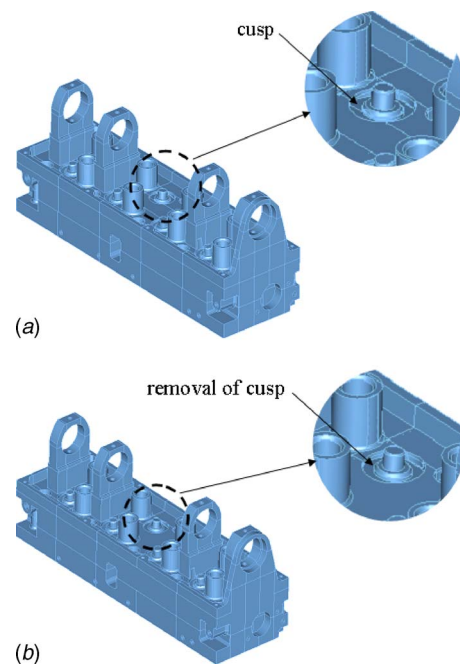
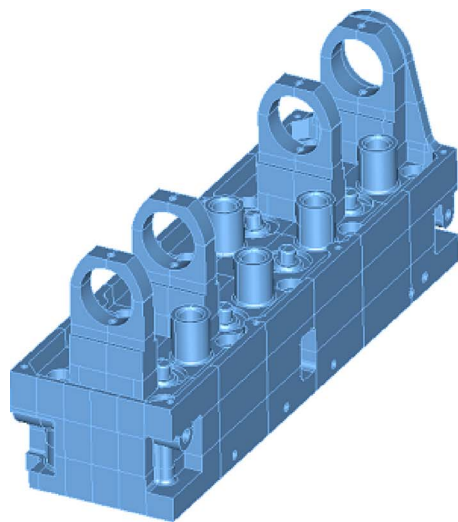
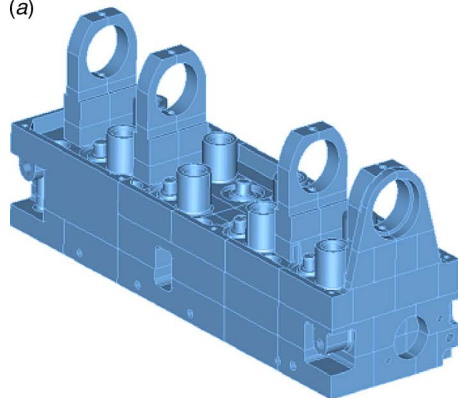


**Fig. 12** Partition refinement for cylinder head with a  $4 \times 4 \times 4$  lattice resolution: (a) before refinement (128 3DUs) and (b) after first refinement (78 3DUs)

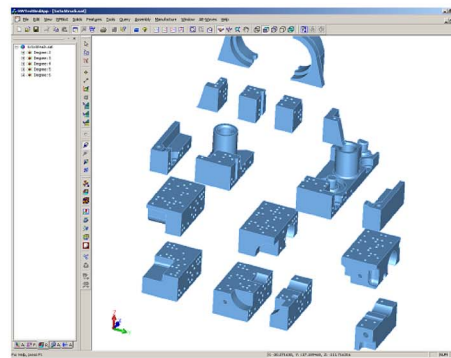




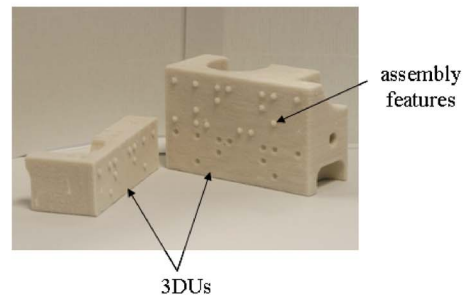
(a)



(b)



(c)



(d)



(e)

**Fig. 13 Prototyping of a cylinder head: (a)  $5 \times 5 \times 5$  lattice partitioning (180 3DUs), (b) refined decomposition (86 3DUs), (c) assembly features generation, (d) 3DU fabrication, and (e) model assembly and final component**

- 1) Characteristic features of the inherent design (e.g., the original part model contains thin sections or shape edges).
- 2) Geometry leading to conflicting requirements (e.g., where merging will remove a thin section but create an oversized 3DU with awkward overhanging features).

The partitioning process does not always generate, automatically, a satisfactory decomposition. The subdivision process nor-

mally creates manufacturable 3DUs, but a small proportion will require manual assessment. Since it is not possible to quantify the algorithm effectiveness in absolute terms, a qualitative assessment may be obtained by observing its behavior over a sample of components with progressively more complex shapes. These components are the castle, truck, and cylinder head. The effectiveness of the refinement strategies is shown in Table 3, which records: (a)



lattice resolution; (b) number of 3DUs generated; (c) DFRP analysis (thin sections TS, cusps CP, and undersized volumes UV); (d) refinement results by the DFRP operators; two optimizations were carried out.

Figure 10 illustrates the refinement process for the castle model with an initial  $5 \times 5 \times 5$  lattice resolution. An initial set of 152 3DUs was created by a lattice of five axis-aligned partitioning planes, as shown in Fig. 10(a). Highlighted in Fig. 10(a) is a 3DU that is typical of those having failed the DFRP assessment due to cusps. Figure 10(b) shows the changes to the 3DU set caused by the DFRP operators, which have successfully modified the partition boundaries to reduce the number of cusps from 76 to 17.

The problem of manufacturing difficulties is well illustrated by the truck component shown in Fig. 11, which corresponds to a partition lattice of  $4 \times 4 \times 4$ . In this case, the three manufacturing problems are present, and the DFRP operators respond by merging 3DUs with their neighbor. Table 3 shows that after the first refinement, the set of 3DUs was reduced from 112 to 83, and the number of thin sections and cusps decreased from 22 to 11 and from 28 to 14, respectively. The removal of a thin section 3DU for this model is highlighted in Fig. 11.

For both the castle and the truck model, a second refinement was carried out, but the results showed that no further reduction of manufacturing problems was achieved. The number of thin sections and cusps remained the same after the second optimization. In these cases, manual inspection by the user is required to evaluate and correct remaining problems with 3DUs, which in most of the cases are related to the initial lattice resolution or the inherent geometry of the component. In the case of the castle component, the cusp problems that the DFRP operators cannot solve would be avoided if a different initial lattice resolution for the castle component (e.g.,  $2 \times 1 \times 5$ ) is defined. In the case of the truck component, the problem features detected (e.g., cusps) arise from the component's design, rather than its subdivision.

Figure 12 illustrates how the system successfully handles numerous DFRP issues found in the initial subdivision of the cylinder head with a  $4 \times 4 \times 4$  lattice. Table 3 reports that thin sections, cusps, and small volumes were decreased considerably in the first optimization, which led to a reduction of 50 3DUs. A second refinement resulted in a further reduction of thin sections and cusps, and in the elimination of small volumes. Because of the complex geometry of the model, further optimizations may result in no reduction of 3DU manufacturing problems.

The order of application of the DFRP operators can affect the final outcome. The functions to remove thin sections and cusps can be sequenced and/or activated individually. Solving for undersized volumes can also be prioritized; for example, the user might want to merge an adjacent 3DU that produces a 3DU with minimum thin sections and cusps.

Having obtained a subdivision that is suitable for manufacture, the AFG operator is applied to generate assembly features to aid the relative location of 3DUs (it is assumed they are secured in place with some form of adhesive). Figure 13 illustrates the decomposition results of the cylinder head shown in Fig. 2. A  $5 \times 5 \times 5$  lattice matrix was used to create 180 3DUs (Fig. 13(a)), which were refined to 86 3DUs using the DFRP operators (Fig. 13(b)). After refining the partition, assembly features were created onto the 3DUs as shown in Fig. 13(c). The STL files for the 3DUs were then generated and used in a ZPrinter 310 machine [33] to fabricate the 3DUs (Fig. 13(d)). Finally the set of 3DUs was assembled to form the complete model, as illustrated in Fig. 13(e).

## 7 Conclusion

The proposed 3DU-RP system automatically generates and refines a decomposition to support the modular prototyping of large-scale physical models using conventional RP systems. For some shapes, the system will be unable to generate a subdivision entirely free of manufacturability problems because of the inherent design of the component, but it is still more efficient than manu-

ally defining the partition boundaries. For this reason, the system's user interface is designed to allow manual review and modification of 3DUs whose manufacturability cannot be improved automatically by the current DFRP operators.

The performance of the system depends on the DFRP operators. Though basic, these operators are capable of generating useful decompositions suited for RP manufacture and the modular architecture of the refinement operators makes the 3DU-RP system extendible. For example, more sophisticated operators can be conceived that incorporate consideration for surface finish and alignment in the build volume. Internal cavities fall out due to the nature of the subdivision process. The surrounding structures (bounding topology and geometry) that form the cavity have to be partitioned into 3DUs. For example, a spherical shell, when sliced generates 3DUs that do not contain any internal voids. Unless an internal cavity was very small in size, then there is the possibility that a 3DU would contain cavity. Again, this can be resolved by selecting a higher lattice resolution, by altering the lattice grid, or even by selectively positioning each individual lattice slicing plane (this option has been built into the GUI).

One weakness of the system is that it attempts to solve problems by addition of 3DUs; never subtraction. Sometimes this strategy can result in 3DUs that are too large. Currently, such oversized 3DUs require manual intervention and reslicing to attempt to generate a better solution. Another limitation of the current implementation is the orientation of the slicing lattice used for the initial subdivision. The authors intend to extend the current system by using a local slicing lattice whose orientation is determined by specific shape features. Some initial work has demonstrated that a combination of feature recognition and surface parameterization can be used to localize and orientate the initial subdivision on components whose features are clearly defined by inner loops of edges. Other researchers have reported techniques that could be adopted to generalize this approach for a broader range of parts [34,35].

Since large components may warp when formed by many RP systems, future work should also consider the evaluation of 3DUs based on a warping analysis to estimate the deflection of the 3DUs when they are produced. If this deflection is bigger than the defined threshold, then the geometry of the 3DU needs to be modified. Some research works on predicting the warping in RP systems are presented in [36,37].

## Acknowledgment

This work was supported by the EPSRC Grant No. GR/R35285/01. The authors also gratefully acknowledge the support of the following industrial partners: BAE Systems, Bridgeport Machines, C.A. Models, Pathtrace, and Renishaw. The first author acknowledges the additional support from the Fund for Research Support (FAI) of the UASLP, México.

## References

- [1] Dutta, D., Brinz, F. B., Rosen, D., and Weiss, L., 2001, "Layer Manufacturing: Current Status and Future Trends," *J. Comput. Inf. Sci. Eng.*, **1**(1), pp. 60–71.
- [2] Henderson, M. R., Kattethota, G., and Roberts, C., 1999, "Manufacturability Evaluation for Rapid Fabrication: A System for Traditional Machining and Layered Manufacturing Planning," *CAD Conference*, Neuchatel, Switzerland, Feb. 22–24.
- [3] Ahn, S. H., McMains, S., Séquin, C. H., and Wright, P. K., 2002, "Mechanical Implementation Services for Rapid Prototyping," *Proc. Inst. Mech. Eng.*, Part B, **216**(8), pp. 1193–1199.
- [4] Binnard, M., and Cutkosky, M. R., 1998, "Building Block Design for Layered Shape Manufacturing," *Proc. of ASME DETC'98*, Paper No. DETC98/DFM-123.
- [5] Hopkinson, N., and Dickens, P., 2001, "Rapid Prototyping for Direct Manufacture," *Rapid Prototyping J.*, **7**(4), pp. 197–202.
- [6] Hague, R., Mansour, S., and Saleh, N., 2003, "Design Opportunities With Rapid Manufacturing," *Assem. Autom.*, **23**(4), pp. 346–356.
- [7] Vasudevarao, B., Natarajan, D. P., and Henderson, M. R., 2000, "Sensitivity of RP Surface Finish to Process Parameter Variation," *Solid Freeform Fabrication Proceedings*, pp. 251–258.
- [8] Wiedemann, B., Dusel, K.-H., and Eschl, J., 1995, "Investigation Into the Influence of Material and Process on Part Distortion," *Rapid Prototyping J.*

- 1(3), pp. 17–22.
- [9] Cheng, W., Fuh, J. Y. H., Nee, A. Y. C., Wong, Y. S., Loh, H. T., and Miyazawa, T., 1995, “Multi-objective Optimization of Part-Building Orientation in Stereolithography,” *Rapid Prototyping J.*, **1**(4), pp. 12–23.
  - [10] Dunne, P., Soe, S. P., Byrne, G., Venus, A., and Wheatley, A. R., 2004, “Some Demands on Rapid Prototypes Used as Master Patterns in Rapid Tooling for Injection Moulding,” *J. Mater. Process. Technol.*, **150**, pp. 201–207.
  - [11] Dolenc, A., and Makela, I., 1994, “Slicing Procedures for Layered Manufacturing Techniques,” *Comput.-Aided Des.*, **26**(2), pp. 119–126.
  - [12] Krause, F. L., Ulbrich, A., Ciesla, M., Klocke, F., and Wirtz, H., 1997, “Improving Rapid Prototyping Processing Speeds by Adaptive Slicing,” *Proc. of the Sixth European Conf. on Rapid Prototyping and Manufacturing*, pp. 31–36.
  - [13] Guduri, S., Crawford, R. H., and Beaman, J. J., 1992, “A Method to Generate Exact Contour Files for Solid Freeform Fabrication,” *Proc. of Solid Freeform Fabrication Symposium*, pp. 95–101.
  - [14] Rajagopalan, M., Aziz, N. M., and Huey, C. O., 1995, “A Model for Interfacing Geometric Modeling Data With Rapid Prototyping Systems,” *Adv. Eng. Software*, **23**, pp. 89–96.
  - [15] Jun, C. S., Kim, D. S., Hwang, J. S., and Chang, T. C., 2000, “Surface Slicing Algorithm for Rapid Prototyping and Machining,” *Proc. of Geometric Modeling and Processing*, pp. 373–382.
  - [16] Smith, T. S., Farouki, R. T., Al-Kandari, M., and Pottmann, H., 2002, “Optimal Slicing of Free-Form Surfaces,” *Comput. Aided Geom. Des.*, **19**, pp. 43–64.
  - [17] Kulkarni, P., Marsan, A., and Dutta, D., 2000, “A Review of Process Planning Techniques in Layered Manufacturing,” *Rapid Prototyping J.*, **6**(1), pp. 18–35.
  - [18] Huang, J., Gupta, S. K., and Stoppel, K., 2003, “Generating Sacrificial Multi-piece Molds Using Accessibility Driven Spatial Partitioning,” *Comput.-Aided Des.*, **35**, pp. 1147–1160.
  - [19] Wang, J., and Ravani, B., 2003, “Computer Aided Contouring Operation for Travelling Wire Electric Discharge Machining (EDM),” *Comput.-Aided Des.*, **35**, pp. 925–934.
  - [20] Chan, C. K., and Tan, S. T., 2005, “Volume Decomposition of CAD Models for Rapid Prototyping Technology,” *Rapid Prototyping J.*, **11**(4), pp. 221–234.
  - [21] Sass, L., 2004, “Design for Self Assembly of Building Components Using Rapid Prototyping,” *ECAADE 2004*, Copenhagen, Denmark.
  - [22] Lim, T., Medellin, H., Corney, J. R., Ritchie, J. M., and Davies, J. B. C., 2004, “Decomposition of Complex Models for Manufacture,” *International Conference on Shape Modeling and Applications*, ACM SMI’04, pp. 337–341.
  - [23] Lim, T., Corney, J. R., Ritchie, J. M., and Davies, J. B. C., 2002, “RPBloX Rapid Prototyping—More Than Just Layers,” *Proc. ASME DETC’02*, Paper No. DETC2002/DFM-34165.
  - [24] Medellin, H., Corney, J. R., Davies, J. B. C., Lim, T., and Ritchie, J. M., 2004, “An Automated System for the Assembly of Octree Models,” *Assem. Autom.*, **24**(3), pp. 297–312.
  - [25] Medellin, H., Corney, J., Davies, J. B. C., Lim, T., and Ritchie, J. M., 2004, “Rapid Prototyping Through Octree Decomposition of 3D Geometric Models,” *Proceedings of the DETC’04 ASME*, Paper No. DETC2004/DFM-57769.
  - [26] Lim, T., Medellin, H., Torres-Sanchez, C., Corney, J. R., Ritchie, J. M., and Davies, J. B. C., 2005, “Edge-Based Identification of DP-Features on Free-Form Solids,” *IEEE Trans. Pattern Anal. Mach. Intell.*, **27**(6), pp. 851–860.
  - [27] Medellin, H., Corney, J., Davies, J. B. C., Lim, T., and Ritchie, J. M., 2006, “Algorithms for the Physical Rendering and Assembly of Octree Models,” *Comput.-Aided Des.*, **38**, pp. 69–85.
  - [28] Gupta, S. K., 1994, “Automatic Manufacturability Analysis of Machined Parts,” Ph.D. thesis, University of Maryland, College Park, MD.
  - [29] Han, J. H., and Han, I., 1999, “Manufacturable Feature Recognition and its Integration With Process Planning,” *Proc. of the 5th ACM Symposium on Solid Modeling and Applications*, pp. 108–118.
  - [30] Brissaud, D., and Tichkiewitch, S., 2000, “Innovation and Manufacturability Analysis in an Integrated Design Context,” *Comput. Ind.*, **43**, pp. 111–121.
  - [31] Chan, C. K., and Tan, S. T., 2003, “Generating Assembly Features Onto Split Solid Models,” *Comput.-Aided Des.*, **35**, pp. 1315–1336.
  - [32] Corney, J. R., and Lim, T., 2001, *3D Modeling With ACIS*, Saxe-Coburg Publications, Stirling, U. K.
  - [33] Z Corporation, Industry-Standard, Three Dimensional Printers and Solutions, <http://www.zcorp.com>
  - [34] Yang, Y., Loh, H. T., Fuh, J. Y. H., and Wong, Y. S., 2003, “Feature Extraction and Volume Decomposition of Orthogonal Layered Manufacturing,” *Comput.-Aided Des.*, **35**, pp. 1119–1128.
  - [35] Ilinkin, I., Janardan, R., Majhi, J., Schwerdt, J., Smid, M., and Sriram, R., 2002, “A Decomposition-Based Approach to Layered Manufacturing,” *Comput. Geom.*, **23**, pp. 117–151.
  - [36] Matsumoto, M., Shiomi, M., Osakada, K., and Abe, F., 2002, “Finite Element Analysis of Single Layer Forming on Metallic Powder Bed in Rapid Prototyping by Selective Laser Processing,” *Int. J. Mach. Tools Manuf.*, **42**, pp. 61–67.
  - [37] Lin, F., and Sun, W., 2001, “Warping Analysis in Laminated Object Manufacturing Process,” *J. Manuf. Sci. Eng.*, **123**(4), pp. 739–753.